



ISSN (Print) : 2320 – 3765  
ISSN (Online): 2278 – 8875

## International Journal of Advanced Research in Electrical, Electronics and Instrumentation Engineering

(An ISO 3297: 2007 Certified Organization)

Website: [www.ijareeie.com](http://www.ijareeie.com)

Vol. 6, Issue 4, April 2017

# Analysis of Time Domain Specifications of a Large Scale PV Integrated Multi Machine Power System using LQR and LQG Control Techniques

Parvathy.G<sup>1</sup>, Manju Sreekumar<sup>2</sup>

M.Tech Student [CS], Dept. of EEE, Mar Baselious College of Engineering and Technology, Trivandrum, India<sup>1</sup>

Assistant Professor, Dept. of EEE, Mar Baselious College of Engineering and Technology, Trivandrum, India<sup>2</sup>

**ABSTRACT:** With increasing electrical power demand, power systems will reach stressed conditions, which leads to undesirable voltage and frequency conditions. Transmission voltage-level photovoltaic (PV) plants are becoming reality in many developed and developing countries around the world. The electricity demand is increasing day by day. The conventional source power plants are failing to meet electric energy demand due to shortage of fuel. This shortfall is being solved by the power generators based on alternative sources (wind, solar, micro-hydro, biomass, geothermal, tidal, etc). To meet the electric power demand, these small capacity power generators are integrated to the power grid. The connection of more number of small and intermediate size generators to power grid at generation and distribution will lead to technical problems like power oscillations, distortion in voltage, harmonics, stability and faults of network. Because of the large integration of photovoltaic plants in to the power system, undesirable phenomenon like power oscillation occurs which leads to the degradation of power quality. In this paper, LQR and LQG controllers are designed to damp out the inter area oscillation in the integrated system. The time domain specifications including the rise time, settling time, overshoot and steady state error are analysed in MATLAB. Simulation results demonstrate that LQG controller has better risetime, settling time, overshoot and steady state error compared to LQR.

**KEYWORDS:** PV plants, Low frequency oscillation (LFO), Power Oscillation Damper, LQG, LQR, Settling Time, Rise Time, Overshoot, Steady State Error

### I.INTRODUCTION

Problems of climate change and energy security cause the increased use of renewable energy sources. Energy related environmental problems can be reduced by using these sources. Renewable energy is the large and inexhaustible source of energy that satisfies power requirements of the world. The most important renewable energy sources are the wind and the photovoltaic. Advantages of photovoltaic generation includes easy installation, low operating and maintenance cost, low emission also the decreasing price of the module due to technological advancement. However, problems associated with PV generation include high initial investment and also intermittency and power quality issues for grid integration. Grid connected PV generation can cause undesirable conditions to power systems, such as high transmission and distribution losses, harmonics, and voltage fluctuations in distribution feeder. Power system stability can be affected by the uncertain natures of PV generation, so it needs to be maintained to provide consistently good quality power to consumers all the time. Large numbers of large scale PV plants are getting integrated into the existing transmission networks nowadays due to the increase in use of renewable energy resources. Majority of the plants and load centers are located geographically far apart and these plants are connected to relatively weak transmission networks. High penetrations of PV on weak transmission link raise possible negative impacts on stability [1]. Large scale PV plants unfavorably affect the low frequency oscillations based upon various factors like the level of penetration, location and control techniques. To damp out the oscillations occurred during interconnection of PV plant



# International Journal of Advanced Research in Electrical, Electronics and Instrumentation Engineering

(An ISO 3297: 2007 Certified Organization)

Website: [www.ijareeie.com](http://www.ijareeie.com)

Vol. 6, Issue 4, April 2017

to grid auxiliary devices like ultra-capacitor, energy storage battery are used due to its intermittent and volatile solar insolation. But increased technology cost limits the large scale application of these devices.

In this paper, analysis of different time domain specifications are done. In order to design LQG controller, state space representation of the entire power system model is required. From that state space matrix, by following a step by step procedure of LQG method, the controller matrix can be formulated. The POD can be used to eliminate the low frequency oscillations. Controller is also designed using LQR method and by comparing the time domain specifications by these two methods, we can see that LQG method provides better time domain specifications.

## II. PHOTOVOLTAIC ARRAY

Solar cell which is a semiconductor device is the basic building blocks of the photovoltaic array. It generates electrical energy by utilizing solar energy. Ideal solar cell has an equivalent characteristic as ideal diode at no illumination. Solar cell performance depends on factors like condition surroundings and solar radiation. Ideal characteristic is not exhibited by commercially accessible solar cells. Photovoltaic generator is based on semiconductor device and solid-state synchronous voltage source converter that resembles a synchronous machine without the rotating part. A balanced set of sinusoidal voltage with rapidly controllable amplitude and phase angle at fundamental frequency is produced. Photovoltaic generator uses voltage source converter to convert a DC input voltage into AC output voltage and it also supplies active and reactive power to the system. Series parallel arrangement of solar cells produces photovoltaic modules which is capable of generating power in Watt range. Photovoltaic array is formed by parallel and series association of those modules which might be used for large applications.

## III. MULTI-MACHINE SYSTEM

In a power system network if a single machine is connected to associate infinite bus or to all completely different machine then it is referred to as single machine infinite bus (SMIB) system. Once over two machines are interconnected throughout a power system network then it is referred to as Multi machine system. In an actual power system, there will be a associate oversized number of load buses and generator buses throughout a multi machine system and it is necessity to maintain the synchronous stability of Multi machine system.

## IV. INTEGRATED SYSTEM

The electric power demand is increasing day by day. But the power plants are failing to meet the electric power demand and is solved by using some alternative energy sources such as wind, solar, geothermal, tides etc... In this paper, photovoltaic modules are integrated to a large scale multi machine power system to meet the electric power demand.

## V. STATE SPACE REPRESENTATION

### A. Modeling of PV

The photovoltaic cells are generally composed of layers of silicon p and silicon n. The light with particular wave length ionizes the atoms of the silicon and the inner field between the positive and negative charges inside the photovoltaic device. The stronger the irradiance, the higher the interaction between the atoms and a higher potential difference is produced. In addition, it is noted that the electrical characteristic of the PV directly depends on the irradiance, which defines an important condition for modeling the PV module. The PVM models normally consist in non-linear equations due to the physical variables involved in the PVM operation. The non-linear models are useful for electrical simulation purposes and energy harvesting evaluation but they introduce a high complexity in terms of control systems analysis and design. The main objective in PV systems is to extract the maximum power available; the PVM must be operated at its MPP. Therefore, three simple modeling approaches are widely accepted in literature [2],[3],[4] to represent the PVM near the MPP: differential resistance, Norton equivalent, and Thevenin equivalent (fig:1).

# International Journal of Advanced Research in Electrical, Electronics and Instrumentation Engineering

(An ISO 3297: 2007 Certified Organization)

Website: [www.ijareeie.com](http://www.ijareeie.com)

Vol. 6, Issue 4, April 2017

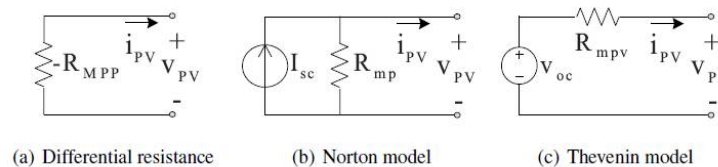


Fig: I PVM linear models around the MPP.

The three linear models accurately represent the PVM electrical behavior at the MPP, but it is noted that the Norton model is closer to the non-linear model for voltages lower than  $V_{MPP}$ .

## State space representation of PV module

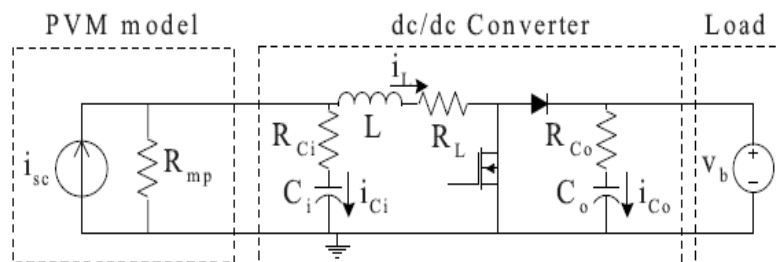


Fig:2 Model considering parasitic losses with voltage-based load.

Where  $i_{sc}$  is the PVM short circuit current,  $R_{mp}$  parallel PVM resistance,  $R_{ci}$  converter input resistance,  $C_i$  converter input capacitor,  $i_{ci}$  converter input current,  $L$  inductor,  $i_L$  inductor current,  $R_L$  converter load resistance,  $R_{co}$  converter output resistance,  $C_o$  converter output capacitor,  $i_{co}$  converter output current,  $V_b$  load side voltage.

The equations that describe the average model of the system are given in (1)–(3). To simplify the expressions, the auxiliary constants defined in (4) are used.

$$\frac{di_L}{dt} = \frac{\beta i_{sc}}{L} + \frac{\lambda V_{ci}}{L} - \frac{\sigma i_L}{L} - V_t \left( \frac{1-d}{L} \right) \quad (1)$$

$$\frac{dV_{ci}}{dt} = \frac{\lambda i_{sc}}{C_i} - \frac{\lambda i_L}{C_i} - \frac{V_{ci}}{C_i (R_{mp} + R_{ci})} \quad (2)$$

$$\frac{dV_{co}}{dt} = \frac{V_b}{C_o R_{co}} - \frac{V_{co}}{C_o R_{co}} \quad (3)$$



## International Journal of Advanced Research in Electrical, Electronics and Instrumentation Engineering

(An ISO 3297: 2007 Certified Organization)

Website: [www.ijareeie.com](http://www.ijareeie.com)

Vol. 6, Issue 4, April 2017

$$\left. \begin{aligned}
 \alpha &= \frac{R_{Co}}{R_{mp} + R_{Co}} \\
 \beta &= \frac{R_{mp} R_{ci}}{R_{mp} + R_{ci}} \\
 \sigma &= \frac{R_{mp} R_{ci}}{R_{mp} + R_{ci}} + R_L \\
 \lambda &= \frac{R_{mp}}{R_{mp} + R_{ci}}
 \end{aligned} \right\} \quad (4)$$

The state space system is now characterized by vectors given in (5) and Jacobian matrices given in (6)–(10).

$$\left. \begin{aligned}
 X &= \begin{bmatrix} i_L \\ V_{ci} \\ V_{co} \end{bmatrix} \\
 U &= \begin{bmatrix} d \\ i_{sc} \\ V_b \end{bmatrix}
 \end{aligned} \right\} \quad (5)$$

Where X is the state vector and U is the input vector. The state matrix A and control matrix B are given by (6) and (7)

$$A = \begin{bmatrix} \frac{-\sigma}{L} & \frac{\lambda}{L} & 0 \\ -\lambda & \frac{1}{L} & 0 \\ \frac{C_i}{L} \frac{V_{ci} \left( \frac{\beta}{R_{mp} + R_{ci}} - \frac{1+d}{L} \right)}{L} & 0 & \frac{-1}{C_o R_{Co}} \\ 0 & \frac{\lambda}{C_i} & 0 \\ 0 & 0 & \frac{1}{C_o R_{Co}} \end{bmatrix} \quad (6)$$

$$B = \begin{bmatrix} 0 \\ 0 \\ \frac{1}{L} \\ 0 \\ 0 \end{bmatrix} \quad (7)$$

The system output, *i.e.*, the PVM voltage, is defined by (8), making C (9) and D (10) matrices different from trivial ones.

$$V_{pv} = \lambda V_{Ci} + \lambda_{iSC} - \lambda R C i_L \quad (8)$$

$$C = [-\beta \quad \lambda \quad 0] \quad (9)$$

$$D = [0 \quad \beta \quad 0] \quad (10)$$

## International Journal of Advanced Research in Electrical, Electronics and Instrumentation Engineering

(An ISO 3297: 2007 Certified Organization)

Website: [www.ijareeie.com](http://www.ijareeie.com)

Vol. 6, Issue 4, April 2017

### B. Modeling of multi-machine system

Multi-machine system consists of four synchronous generators related to four 20/230-kV step-up transformers. All generators with in the system consist of exciter and governor. Standard PSS has been enclosed in generator excitation system. An aggregated PV plant is connected to the grid. Here are two load buses in the system: Load 1 consists of 1767 MW and 100 MVar, whereas Load 2 consists of 967 MW and 100 MVar. System loads are considered as constant power  $P$  load. The test system consists of two absolutely symmetrical areas linked together by two 230 kV lines of 220 km length. It was specifically designed to review low frequency oscillations in massive interconnected power systems. Despite its small size, it mimics very closely the behavior of typical systems in actual operation. Each area is equipped with two identical round rotor generators rated 20 kV/900 MVA. The synchronous machines have identical parameters except for inertias. Thermal plants having identical speed regulators are further assumed in any respect locations, in addition to quick static exciters.

The state space representation of multi machine system is represented by equation (11)- (19)

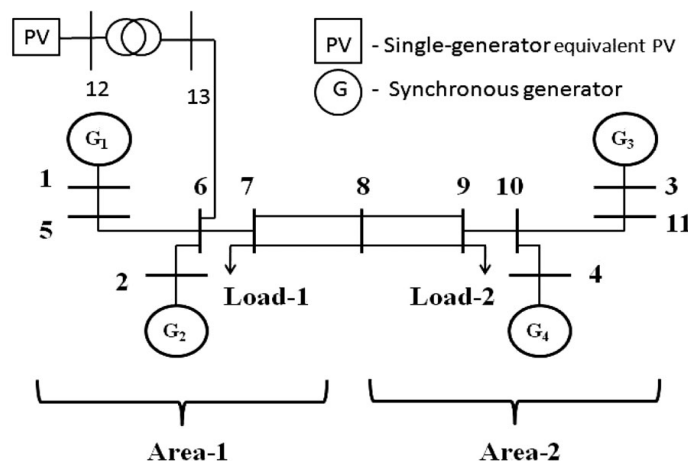


Fig:3 single line diagram of Multi machine test system

$$\dot{x}_1 = \frac{-1}{T_{P1}} x_1 + \frac{K_{P1}}{T_{P1}} x_2 - \frac{K_{P1}}{T_{P1}} x_7 - \frac{K_{P1}}{T_{P1}} d_1 \quad (11)$$

$$\dot{x}_2 = \frac{x_3 - x_2}{T_{t1}} \quad (12)$$

$$\dot{x}_3 = \frac{1}{T_{g1}} \left[ \frac{-1}{R_1} x_1 + u_1 - x_3 \right] \quad (13)$$

$$\dot{x}_4 = \frac{1}{T_{P2}} \left[ K_{P2} (x_5 + x_7 - d_2) - x_4 \right] \quad (14)$$

$$\dot{x}_5 = \frac{1}{T_{g2}} \left[ \frac{-1}{R_2} x_2 + u_2 - x_5 \right] \quad (15)$$

$$\dot{x}_6 = \frac{1}{T_{t2}} \left[ \frac{-1}{R_2} x_2 + u_2 - x_6 \right] \quad (16)$$

$$\dot{x}_7 = 2\pi T^0 x_1 - 2\pi T^0 x_4 \quad (17)$$

$$\dot{x}_7 = 2\pi T^0 x_1 - 2\pi T^0 x_4 \quad (18)$$

$$\dot{x}_7 = 2\pi T^0 x_1 - 2\pi T^0 x_4 \quad (19)$$



## International Journal of Advanced Research in Electrical, Electronics and Instrumentation Engineering

(An ISO 3297: 2007 Certified Organization)

Website: [www.ijareeie.com](http://www.ijareeie.com)

Vol. 6, Issue 4, April 2017

$$\dot{x}_8 = B_1 x_1 + x_7$$

$$\dot{x}_9 = B_2 x_4 - x_7$$

Where, X(9x1) is the state vector, U(2x1) control vector, and d(2x1) disturbance vector,  $\Delta f_1$  &  $\Delta f_2$  : Frequency Deviations in Areas 1 & 2,  $\Delta P_{tie(1,2)}$  : Tie Line Power Deviation in Two Areas Systems,  $R_1$  &  $R_2$  : Regulations of Governors in Areas 1, 2,  $K_T$  : Integral Controller Gain in Thermal Areas,  $K_H$  : Integral Controller Gain in Hydro Area,  $u_1$  &  $u_2$  : Control Inputs in Areas 1 & 2,  $\Delta P_{g1}$  &  $\Delta P_{g2}$  : Deviations in Governor Power Outputs in Thermal Areas 1 & 2,  $\Delta P_{G1}$  : Deviation in Governor (stage 1) Power Output in Hydro Area,  $\Delta P_{G2}$  : Deviation in Governor (stage 2) Power Output in Hydro Area,  $\Delta P_{t1}$  &  $\Delta P_{t2}$  : Deviations in Turbine Power Outputs in Thermal Areas 1 & 2,  $\Delta P_{D1}$  &  $\Delta P_{D2}$  : Load Disturbances in Areas 1 & 2,  $K_{P1}$  &  $K_{P2}$  : Power System Constants in Areas 1 & 2,  $T_{P1}$  &  $T_{P2}$  : Power System Time Constants in Areas 1 & 2,  $B_1$  &  $B_2$  : Tie Line Frequency Bias in Areas 1 & 2,  $T_0$  : Synchronizing Coefficient for Tie Line for Two Area Systems,  $T_{12}$  : Synchronizing Coefficients for Tie Lines between Pair of Areas, For the Two-Area System,  $T_{g1}$  &  $T_{g2}$  : Governor Time Constants for Thermal Areas 1 & 2,  $T_{t1}$  &  $T_{t2}$  : Turbine Time Constants for Thermal Areas 1 & 2,  $a_{12}$  : Ratio of Rated Powers of a Pair of Areas in the Two Area System

### C. Modeling of integrated system

Transfer function of integrated system is given by

$$S = \frac{13535S^4 + 2.028 \times 10^5 S^3 + 3.683 \times 10^5 S^2 + 2.458 \times 10^5 S + 5.978 \times 10^4}{S^8 + 4.074 \times 10^4 S^7 + 1.47 \times 10^6 S^6 + 2.103 \times 10^7 S^5 + 1.345 \times 10^8 S^4 + 3.331 \times 10^8 S^3 + 8.696 \times 10^8 S^2 + 5.456 \times 10^8 S + 5.369 \times 10^8} \quad (20)$$

The state space representation of integrated system is represented by

$$\dot{x} = Ax + Bu \quad (21)$$

$$Y = Cx + Du \quad (22)$$

Where A, B, C, D matrices are

$$A = \begin{pmatrix} -40740 & -1470000 & -21030000 & -134500000 & -333100000 & -869600000 & -545600000 & -5369000 \\ 1 & 0 & 0 & 0 & 0 & 0 & 0 & 0 \\ 0 & 1 & 0 & 0 & 0 & 0 & 0 & 0 \\ 0 & 0 & 1 & 0 & 0 & 0 & 0 & 0 \\ 0 & 0 & 0 & 1 & 0 & 0 & 0 & 0 \\ 0 & 0 & 0 & 0 & 1 & 0 & 0 & 0 \\ 0 & 0 & 0 & 0 & 0 & 1 & 0 & 0 \\ 0 & 0 & 0 & 0 & 0 & 0 & 1 & 0 \\ 0 & 0 & 0 & 0 & 0 & 0 & 0 & 1 \end{pmatrix}$$

$$B = [1 \ 0 \ 0 \ 0 \ 0 \ 0 \ 0 \ 0]^T$$

$$C = [0 \ 0 \ 0 \ 13535 \ 202800 \ 368300 \ 245800 \ 59780]$$

$$D = [0]$$

### VI. CONTROLLER DESIGN



# International Journal of Advanced Research in Electrical, Electronics and Instrumentation Engineering

(An ISO 3297: 2007 Certified Organization)

Website: [www.ijareeie.com](http://www.ijareeie.com)

Vol. 6, Issue 4, April 2017

## A.OPTIMAL LQR CONTROL DESIGN

The objective of the optimal control design is determining the optimal control law  $u(t,x)$  which can transfer system from its initial state to the final state such that given quadratic performance index is minimized.

The command used for LQR design is

$$[K] = \text{lqr}(A,B,Q,R) \quad (23)$$

Q is positive semi definite matrix and R is real symmetrical matrix. The problem is to find the vector feedback K of control law, by choosing matrix Q and R to minimize the quadratic performance index J is described by

$$J = \int_0^{\infty} (\square x' Q \square x + \square u' R^{-1} \square u) dt \quad (24)$$

Where  $Q = p * C' * C$  and R is selected as same as that of the order of B matrix

## B.OPTIMAL COMPENSATOR LQG CONTROL

We have introduced the Kalman filter, which is an optimal observer for multi-output plants in the presence of process and measurement noise, modeled as white noises. The optimal compensator Linear Quadratic Gaussian (LQG) consists of combination between optimal LQR control and Kalman filter .In short, the optimal compensator LQG design process is the following:

- (1) Design an optimal regulator LQR for a linear plant assuming full-state feedback (i.e. assuming all the state variables are available for measurement) and a quadratic objective function.
- (2) Design a Kalman filter for the plant assuming a known control input,  $u(t)$ , a measured output,  $y(t)$ , and white noises,  $v(t)$  and  $z(t)$ . The Kalman filter is designed to improve an optimal estimate of the state-vector.
- (3) Combine the separately designed optimal regulator LQR and Kalman filter into an optimal compensator LQG.
- (4) The optimal regulator feedback gain matrix, K, and the Kalman filter gain matrix, L, are used to complete closed compensator system LQG .The command used for design LQG controller is

$$L = \text{lqe}(A,\text{eye}(n),C,W,V); \quad (25)$$

## VII. SIMULATION RESULTS

The simulation of the whole system is done in MATLAB.The formation of state space matrices and the design of controller is done by using MATLAB programming. Then it is incorporated to the system and analyzed that oscillations are reduced. The entire system has to be represented in state space format so that it can be given as input to the controller.x is the system state vector of dimension n (64) ,y is the output vector of dimension p (8) ,u is the input vector of dimension m (8) ,A is the state matrix of size  $n \times n$  (64x64) ,B is the input matrix of size  $n \times m$  (64x8) , C is the output matrix of size  $p \times n$  (8x64) , D is the feed-forward matrix of size  $p \times m$ . (8x8).Eigen value analysis is done to find out the damping factors and frequency for a particular mode . Therefore we can easily identify which are the modes to be damped. By following the design criteria LQR and LQG controller matrix is obtained. Reduced order controller matrix is obtained. A matrix or the state matrix is of order 8x8. B matrix or the input matrix is of order 8x1. C matrix is of order 1x8. The D matrix is a null matrix which is of order 1x1. Similarly a different controller matrix is obtained for LQG method also. The designed controller is incorporated into the system so that oscillations are reduced. A 3–5 settling time is adopted by many utilities in their system design and operational guidelines.



# International Journal of Advanced Research in Electrical, Electronics and Instrumentation Engineering

(An ISO 3297: 2007 Certified Organization)

Website: [www.ijareeie.com](http://www.ijareeie.com)

Vol. 6, Issue 4, April 2017

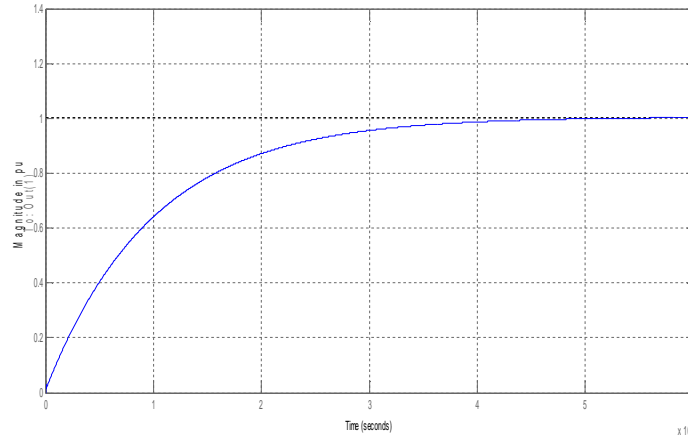


Fig:4 closed loop step response -LQG

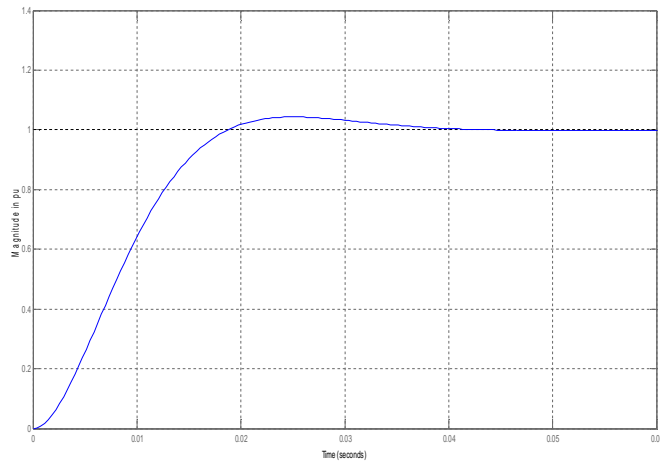


Fig:5 closed loop step response-LQR

It is evident from the obtained results(fig:4&fig:5) that overshoot,steady state error as well as rise time is reduced in the case of LQG method when compared to LQR.

Integrated system	Overshoot (%)	Rise time (sec)	Steady state error	Settling time
System with LQR	4.3	$2.19 \times 10^{-4}$	0.999684	$3.89 \times 10^{-4}$
System with LQG	0	0.0121	0.999684	0.0335

Table:1 comparison of LQR and LQG in integrated system





ISSN (Print) : 2320 – 3765

ISSN (Online): 2278 – 8875

# International Journal of Advanced Research in Electrical, Electronics and Instrumentation Engineering

(An ISO 3297: 2007 Certified Organization)

Website: [www.ijareeie.com](http://www.ijareeie.com)

Vol. 6, Issue 4, April 2017

## VIII.CONCLUSION

This work demonstrated the possibility of using a damping controller at a PV plant to effectively damp out the inter-area oscillation resulting in a interconnected power grid. A systematic approach of designing POD based on the LQR and LQG technique is described here. The state space representation of the entire system is formulated. A reduced-order model of the designed controller is used to verify its performance for inter-area oscillation damping and also the time domain specifications were analysed.

## REFERENCES

- [1] Y. T. Tan, "Impact of power system with a large penetration of photovoltaic generation," Ph.D. dissertation, Inst. of Sci. and Technol. The Univ. Of Manchester, Manchester, U.K., 2004
- [2] Petrone, G.; Spagnuolo, G.; Vitelli, M. Analytical model of mismatched photovoltaic fields by means of Lambert W-function. Sol. Energy Mater. Sol. Cells 2007, 91, 1652–1657
- [3] Petrone, G.; Ramos-Paja, C. Modeling of photovoltaic fields in mismatched conditions for energy yield evaluations. Electr. Power Syst. Res. 2011, 81, 1003–1013.
- [4] Yau, H.T.; Wu, C.H. Comparison of Extremum-Seeking Control Techniques for Maximum Power Point Tracking in Photovoltaic Systems. Energies 2011, 4, 2180–2195.
- [5] P. Kundur. Power System Stability and Control. McGraw-Hill, New York, 1994.
- [6] R. Shah, N. Mithulananthan, A. Sode-Yome, and K. Y. Lee, "Impact of large-scale PV penetration on power system oscillator. stability," in Proc. IEEE Power Energy Soc. General Meeting, Minneapolis, MN, Jul. 25–29, 2010, pp. 1–7
- [7] M. G. Villalva, J. R. Gazoli, and E. R. Filho, "Comprehensive approach to modeling and simulation of photovoltaic arrays," IEEE Trans. Power Electron., vol. 24, no. 5, pp. 1198–1208, May 2009.
- [8] R. Shah, N. Mithulananthan, and K. Y. Lee, "Contribution of PV systems with ultra-capacitor energy storage on inter-area oscillation," in Proc. IEEE Power Energy Soc. General Meeting, Detroit, MI, Jul. 24–28, 2011, pp. 1–8.
- [9] Bellini, A.; Bifaretti, S.; Iacovone, V.; Cornaro, C. Simplified model of a photovoltaic module. Energia Solare Test Ricerca ESTER Publ. 2009, 1, 1–5.
- [10] M Ghandhari, G Andersson. "Damping of inter-area and local modes by the use of controllable components", IEEE Transaction on Power Delivery, 2007; 10(4).